Evaporation–Precipitation Variability over the Mediterranean and the Black Seas from Satellite and Reanalysis Estimates

A. ROMANOU AND G. TSELIOUDIS

Department of Applied Mathematics and Applied Physics, Columbia University, and NASA GISS, New York, New York, and Centre for Atmospheric Physics and Climatology, Academy of Athens, Athens, Greece

C. S. ZEREFOS

Department of Geology, University of Athens, and Centre of Atmospheric Physics and Climatology, Academy of Athens, Athens, Greece

C.-A. CLAYSON

Department of Meteorology, The Florida State University, Tallahassee, Florida

J. A. CURRY

School of Earth and Atmospheric Sciences, Georgia Institute of Technology, Atlanta, Georgia

A. ANDERSSON

Meteorological Institute, University of Hamburg, Hamburg, Germany

(Manuscript received 16 November 2009, in final form 30 March 2010)

ABSTRACT

Satellite retrievals of surface evaporation and precipitation from the Hamburg Ocean Atmosphere Parameters and Fluxes from Satellite Data (HOAPS-3) dataset are used to document the distribution of evaporation, precipitation, and freshwater flux over the Mediterranean and Black Seas. An analysis is provided of the major scales of temporal and spatial variability of the freshwater budget and the atmospheric processes responsible for the water flux changes. The satellite evaporation fluxes are compared with fields from three different reanalysis datasets [40-yr ECMWF Re-Analysis (ERA-40), ERA-Interim, and NCEP].

The results show a water deficit in the Mediterranean region that averages to about 2.4 mm day^{-1} but with a significant east–west asymmetry ranging from 3.5 mm day^{-1} in the eastern part to about 1.1 mm day^{-1} in the western part of the basin. The zonal asymmetry in the water deficit is driven by evaporation differences that are in turn determined by variability in the air–sea humidity difference in the different parts of the Mediterranean basin. The Black Sea freshwater deficit is 0.5 mm day^{-1}, with maxima off the northern coast (0.9 mm day^{-1}) that are attributed to both evaporation maxima and precipitation minima there.

The trend analysis of the freshwater budget shows that the freshwater deficit increases in the 1988–2005 period. The prominent increase in the eastern part of the basin is present in the satellite and all three reanalysis datasets. The water deficit is due to increases in evaporation driven by increasing sea surface temperature, while precipitation does not show any consistent trends in the period. Similarly, in the Black Sea, trends in the freshwater deficit are mainly due to evaporation, although year-to-year variability is due to precipitation patterns.

1. Introduction

Recent observational analyses of twentieth-century Mediterranean precipitation trends show large decreases in the Mediterranean region (Giorgi 2002; Luterbacher et al. 2006), while modeling studies predict a continuation of those decreases into the twenty-first century (Raisanen 2002). Emphasis in those studies has been given to the analysis of precipitation trends and variability. However, in order to obtain an understanding of the processes involved in determining the variability of

Corresponding author address: Anastasia Romanou, Columbia University, 2880 Broadway, New York, NY 10025.
E-mail: ar2235@columbia.edu

DOI: 10.1175/2010JCLI3525.1

© 2010 American Meteorological Society

the regional water budget, it is important to resolve all components of that budget as well as the variability of the atmospheric processes that affect those components. In the Mediterranean region, freshwater fluxes at the sea surface [i.e., the difference between evaporation and precipitation ($E - P$) provide the major source of water to the atmospheric hydrologic cycle (Mariotti et al. 2002). Long-term variability of $E - P$ over the Mediterranean Sea will determine to a large extent the variability of freshwater deficit and consequently variability in the hydrography of the region and the Mediterranean outflow into the Atlantic Ocean. Similarly, over the Black Sea freshwater fluxes (together with river outflow) are known to set the barotropic component of the Dardanelles throughflow that affects the hydrographic properties and the deep water convection in the Aegean Sea (Staneva and Stanev 1998).

Freshwater flux variability can result from changes in dynamic or thermodynamic atmospheric conditions and recently special attention has been placed to potential changes in a warming climate with respect to the location and strength of midlatitude storm tracks (Bengtsson et al. 2006). At the same time, surface water and momentum fluxes drive overturning and affect the basin ocean circulation. Evidence for the relocation of the Mediterranean Deep Water (MDW) source from the Aegean Sea to the Adriatic Sea is associated with changes in the surface forcing (Rubino and Hainbucher 2007; Josey 2003).

The water cycle is among the most uncertain aspects of climate model predictions because of uncertainty in modeling of the precipitation and evaporation fields. However, uncertainty estimates are hard to obtain because of the lack of large-scale, sufficiently long measurements of both, especially the latter. Our knowledge of the freshwater budget over the Mediterranean is largely dependent on in situ measurements of limited spatial and temporal resolution and on reanalysis estimates (Peixoto et al. 1982; Boukthir and Barnier 2000; Mariotti et al. 2002). Reanalysis methods depend on the assimilation of in situ measurements along with some satellite retrievals, but they model most of the parameters that are involved in the water cycle and hence depend on model parameterizations. In the last few decades, satellite instruments have been used to determine the components of the sea surface energy budget (e.g., Curry et al. 2004). These retrievals have sufficient spatial and temporal coverage to deduce useful conclusions about the variability of the water cycle in the Mediterranean Sea at seasonal and interannual scales; however, their accuracy has not been hitherto evaluated in the region. The present study introduces the satellite estimates and compares them with both reanalysis and in situ measurements directly and through comparisons with earlier works (e.g., Mariotti et al. 2002).

The objective of the present work is to use satellite retrievals of surface freshwater fluxes to map the distribution of freshwater fluxes over the Mediterranean basin, compare them to the reanalysis fluxes, determine their major scales of time and space variability, and examine the atmospheric processes that are responsible for the water flux changes. The analysis focuses on precipitation and evaporation changes at some distance from the Mediterranean coastline, since satellite estimates are most reliably retrieved there (Grassl et al. 2000). As a result, the present analysis does not fully close the Mediterranean water budget, nor it is intended to, as that would require the inclusion of the coastal regions and of river runoff estimates.

In the paper, section 2 describes the major characteristics and relevant aspects of the satellite and reanalysis datasets that are used in this work. The mean climatology and variance of the freshwater cycle in the Mediterranean Sea, derived from satellite retrievals, is described in section 3, and four subbasins with distinct climatological characteristics are identified for further analysis. Section 4 describes the major scales of temporal variability for all components of the surface water budget from satellite and reanalysis data, for each of the subbasins. Finally, a synopsis and discussion of the main points derived from the analysis are presented in section 5.

2. Datasets

a. The HOAPS-3 dataset

Satellites retrieve atmospheric parameters at global scales that allow the derivation of global time series of surface energy fluxes. The freshwater flux and the related energy fluxes at the air–sea interface are, however, among the most challenging parameters to be estimated from satellite measurements. Based on carefully constructed and validated algorithms applied to satellite data, the Hamburg Ocean Atmosphere Parameters and Fluxes from Satellite Data (HOAPS-3; Andersson 2009) provides a state-of-the-art global climatology of sea surface evaporation and precipitation as well as the related sea surface and atmospheric state parameters. The dataset further includes the sea surface and atmospheric parameters that are used to estimate surface evaporative flux, such as wind speed, sea surface temperature (SST), air humidity, and air–sea humidity difference. Except for the SST, all variables are derived from Special Sensor Microwave Imager (SSM/I) passive microwave satellite radiances over the ice-free global ocean. The flux products from HOAPS3 have been evaluated with good results against other satellite based as well as in situ flux products (Chou et al. 2004; Bourras 2006).

HOAPS-3 contains a neural network based precipitation algorithm—the National Oceanographic Data Center (NODC)–Rosenstiel School of Marine and Atmospheric Science (RSMAS) Advanced Very High Resolution Radiometer (AVHRR) Oceans Pathfinder SST product (see http://www.nodc.noaa.gov/SatelliteData/pathfinder4km/)—that relies on temperature measurements from National Oceanic and Atmospheric Administration (NOAA) polar orbiting satellites. This new procedure to synthesize the 85-GHz brightness temperatures was employed during the time period (April 1988–December 1991) that for the SSM/I on the Defense Meteorological Satellite Program (DMSP) satellite *DMSP-F08* was defective. A new twice-daily gridded data product of the surface latent heat flux (LH) is calculated using a bulk aerodynamic formula (following Fairall et al 1996). In this formula latent heat flux is a product of the wind speed and the difference between the surface saturation humidity at sea and the surface air humidity:

$$\mathrm{LH} = \rho L v C_E V_s (q_s - q_a),$$

where V_s is the surface wind at 10 m, q_a is the surface (2 m) air specific humidity, C_E is the exchange coefficient for latent heat flux, and q_s is the saturation specific humidity at sea surface pressure and SST. In HOAPS-3 surface wind speed and air humidity are obtained from SSM/I retrievals. Sea surface saturation humidity comes from a Magnus formula applied to the SST field.

The spatial resolution of the dataset that is used in this study is 0.5° and the temporal resolution is monthly for the period from January 1988 to December 2005, covering 18 full years. The study focuses on the retrievals of evaporation and precipitation that constitute the freshwater budget at the sea surface, as well as the retrievals of wind, SST, and air–sea humidity difference that are used in a bulk formula to calculate the evaporation values (Fairall et al. 1996).

SSM/I retrievals are difficult if not impossible near the coast and over island regions where contamination by emissions from land is significant; accordingly, this study concentrates on the open water areas of the basin. This topic will be discussed in section 5.

b. *ERA-40 and ERA-Interim*

The 40-yr European Centre for Medium-Range Weather Forecasts (ECMWF) Re-Analysis (ERA-40; Uppala et al. 2005) produced a comprehensive set of global analyses describing the state of the atmosphere, land, and ocean wave conditions starting in 1957. The ERA-40 project applies a modern variational data assimilation technique (used in daily operational numerical forecasting at ECMWF) to the past conventional and satellite observations to produce a global atmospheric dataset with 3-hourly time resolution and 2.5° horizontal resolution. With respect to the parameters relevant to surface energy fluxes, the ERA-40 dataset assimilates SSM/I radiance measurements. The use of SSM/I radiances involves a one-dimensional variational analysis of the total column water content and surface wind speed. Sea surface temperature is specified from a variety of conventional observations, and surface humidity values come from both conventional observations and the use of Television and Infrared Observation Satellite (TIROS) Operational Vertical Sounder (TOVS) radiances in the assimilation system.

The ERA-Interim dataset is the latest reanalysis dataset released by ECMWF (Berrisford et al. 2009) that focuses on the data-rich period since 1989. At 1.5° horizontal resolution, it includes many model improvements, the use of four-dimensional variational analysis, a revised humidity analysis, variational bias correction for satellite data, and other improvements in data handling. ERA-Interim uses mostly the sets of observations acquired for ERA-40, supplemented by data for later years from ECMWF's operational archive. There are a few new observational datasets that are introduced and some of those, such as the reprocessed winds and clear-sky radiances, may have an effect on the surface energy fluxes examined in this study.

c. *NCEP–NCAR reanalysis*

The National Centers for Environmental Prediction (NCEP)–National Center for Atmospheric Research (NCAR) Reanalysis Project [described in more detail in Kalnay et al. (1996)] includes the NCEP global spectral model operational in 1995, with 28 ''sigma'' vertical levels and a horizontal triangular truncation of 62 waves, equivalent to about 210 km (about 1.9°). The analysis scheme is a three-dimensional variational data assimilation (3DVAR) scheme cast in spectral space denoted spectral statistical interpolation. The assimilated observations include upper air rawinsonde observations of temperature, horizontal wind, and specific humidity; operational TOVS vertical temperature soundings from NOAA polar orbiters over ocean, with microwave retrievals excluded between 20°N and 20°S because of rain contamination; temperature soundings over land; cloud tracked winds from geostationary satellites; aircraft observations of wind and temperature; land surface reports of surface pressure; and oceanic reports of surface pressure, temperature, horizontal wind and specific humidity.

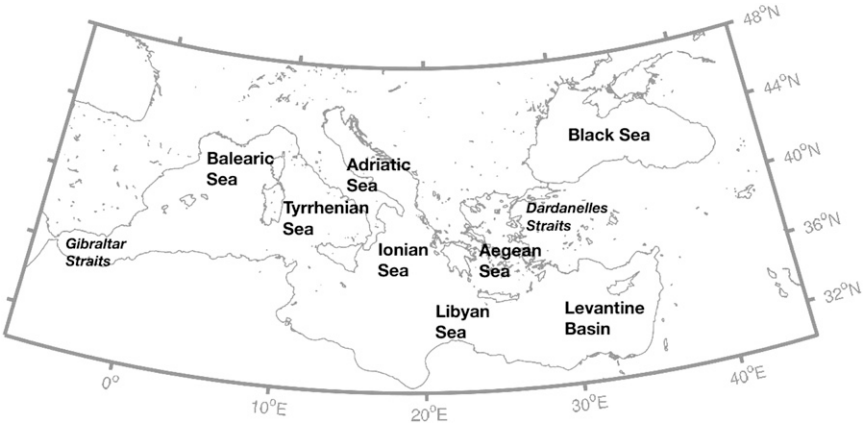

FIG. 1. Geography of the Mediterranean Sea basin and subbasins and the Black Sea.

3. Freshwater budget climatology

Strictly speaking, the term ''freshwater budget'' in the Mediterranean includes, in addition to evaporation and precipitation, the continental and riverine runoff and the water exchanges through the major straits of Gibraltar and Dardanelles (Fig. 1). Here, the term denotes the difference between evaporation and precipitation ($E - P$).

a. Freshwater budget, evaporation, and precipitation

The HOAPS-3 estimated climatological average freshwater budget for the Mediterranean and the Black Seas over the period 1988–2005 (Fig. 2a) is characterized by mostly positive values, implying excessive evaporation over the precipitation throughout the basin with negative values occurring only over the Black Sea. Freshwater budget maxima occur in the eastern Mediterranean Levantine basin at about 3.5 mm day^{-1} and minima in the western basin at about 1.5 mm day^{-1}. The central Mediterranean basin exhibits a 1.5–2.5 mm day^{-1} loss of freshwater. The largest variability due to interannual changes (Fig. 2b) occurs in the northern Ionian Sea (up to 2.4 mm day^{-1}) south of the Otranto Straits, in between southern Italy and Sicily and off western continental Greece, the Gulf of Lions (1.6 mm day^{-1}), and the western Black Sea (2–2.4 mm day^{-1}).

On average, the Black Sea loses freshwater at a rate of 0.5 mm day^{-1} mainly at the easternmost and westernmost edges of it; however, interannual changes (1.7 mm day^{-1}) especially in the west are large. In the following the mean state of the freshwater balance will be described and discussion on uncertainties will be given at the end of the section. This value is fairly close to Unluata et al.'s estimates (0.4 mm day^{-1}) as reported in Staneva and Stanev (1998).

The geographical distribution of the freshwater budget follows that of basinwide evaporation (Fig. 2c) and precipitation reinforces that dependence (Fig. 2e) since precipitation is least where evaporation is largest (i.e., in the eastern basin). Maximum evaporation occurs in the Levantine basin (about 4 mm day^{-1}) and minimum evaporation in the western Mediterranean (about 2.2 mm day^{-1}) and the easternmost Black Sea (about 1.5 mm day^{-1}). Precipitation extremes are reversed, with minimum values on the eastern and southernmost parts of the Mediterranean basin (0.2–0.4 mm day^{-1}) and maximum ones in the northern Ionian Sea (1.4 mm day^{-1}) and the westernmost Black Sea (up to 2 mm day^{-1}; Fig. 2e).

Evaporation over the Ionian waters is nearly uniform, with values ranging from 3 mm day^{-1} in the northern part of the basin near the Straits of Otranto to 3.5 mm day^{-1} near the Libyan coast. Precipitation, however, exhibits a preferentially zonal structure with the largest values occurring in the northern Ionian Sea (1.4 mm day^{-1}) south of the Straits of Otranto, although the interannual variability of this signal is also the largest in the basin (about 2.3 mm day^{-1}; Fig. 2f). The freshwater budget in the Ionian basin is mainly controlled by the rainfall patterns in the region rather than the evaporation, which is mostly uniform.

The Levantine, on the other hand, is a persistently dry region, since both the mean precipitation and its variability are low. The western Mediterranean variability patterns in the evaporation and rainfall (Figs. 2d,f) are such that evaporation variability maxima coincide with precipitation minima and therefore cancel out in their contribution to freshwater budget. As a result moderate freshwater loss variability patterns occur throughout the observation period (Fig. 2b).

The Black Sea loses on average 1.8 ± 1.1 mm day^{-1} freshwater through evaporation and gains 1.3 ± 0.9 mm day^{-1} through precipitation, with maximum precipitation occurring off the western coast. Unluata et al.

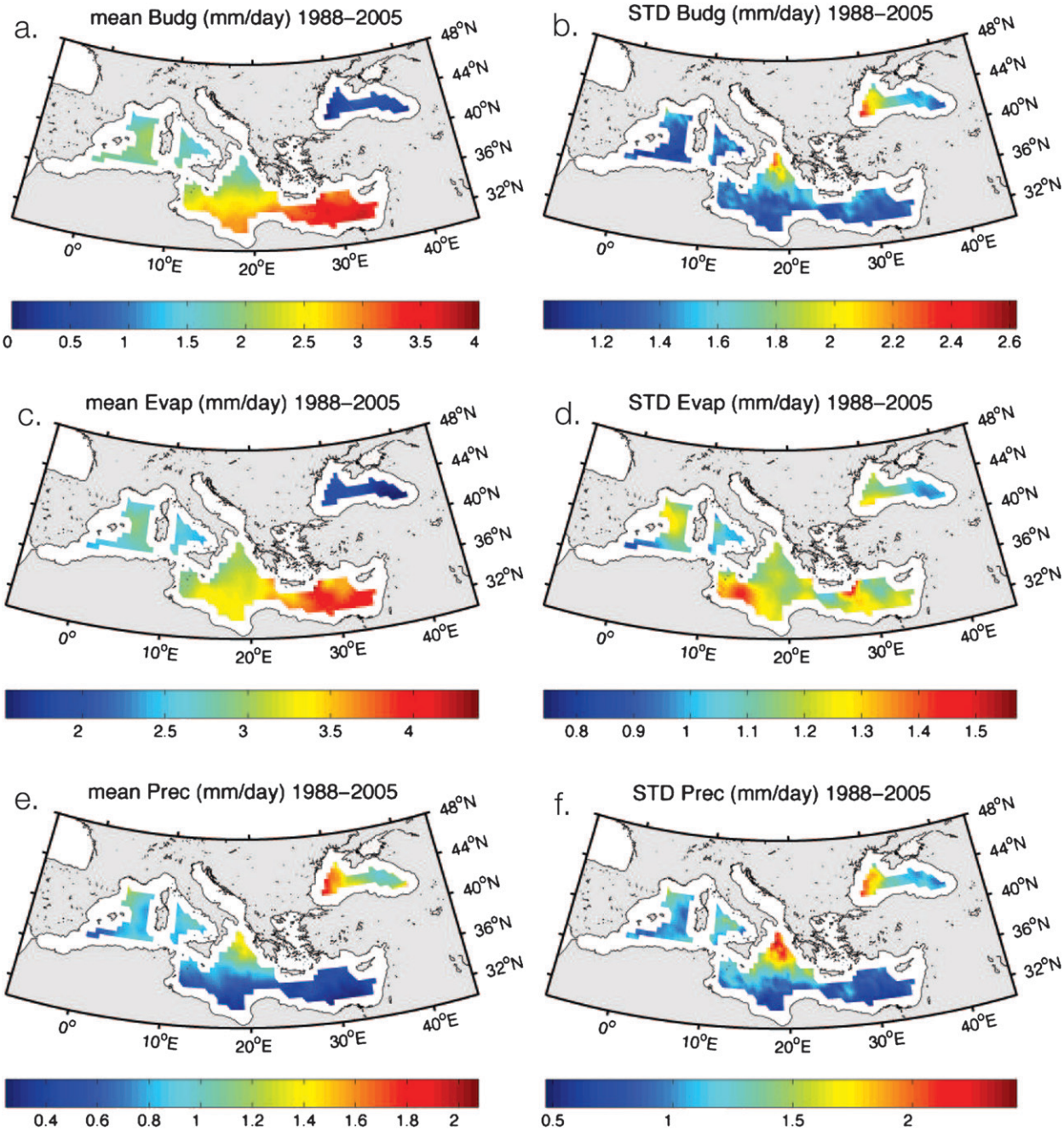

FIG. 2. HOAPS-3 climatologies: (left) mean state and (right) interannual variability (std dev) for the period 1988–2005. (a),(b) Freshwater budget ($E - P$), (c),(d) evaporation, and (e),(f) precipitation (all in mm day^{-1}).

[as reported in Staneva and Stanev (1998)] give 2.3 and 1.9 mm day^{-1} rates for evaporation and precipitation, respectively.

The basinwide annual mean values from the HOAPS-3 dataset are 1037 mm yr^{-1} for evaporation, 292 mm yr^{-1} for precipitation, and 745 mm yr^{-1} for the freshwater budget. The evaporation estimate ranks the satellite value in the middle of the range of values derived in previous studies. Observational studies, that derive climatological estimates based on surface marine reports from ships, buoys, and other platform types tend to have higher evaporation values that range from 1120 to 1150 mm yr^{-1} (Gilman and Garrett 1994; Castellari et al. 1998; Béthoux and Gentili 1999; Mariotti et al. 2002). Reanalysis estimates using both NCEP and ERA datasets, on the other hand, report values ranging between 920 and

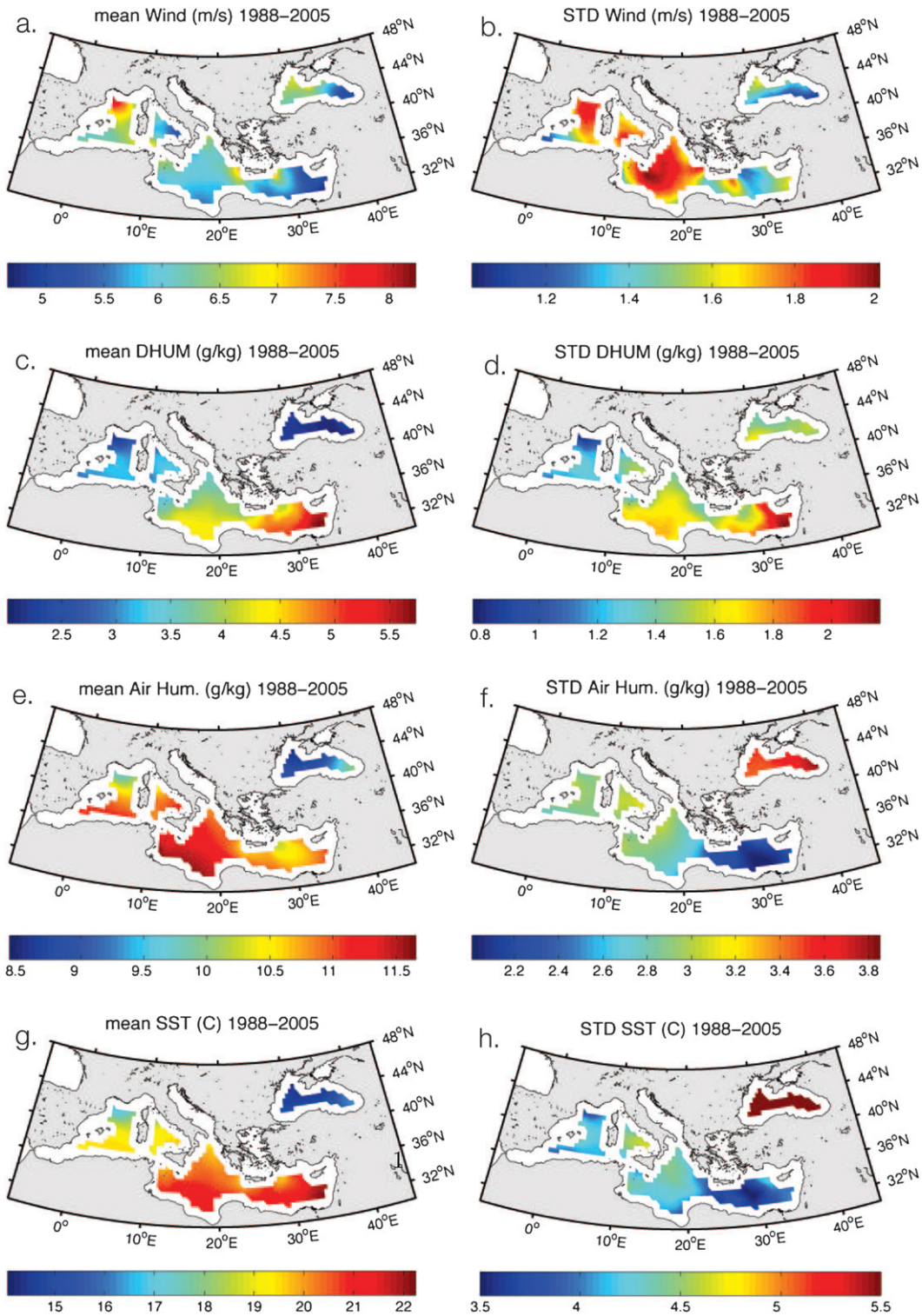

FIG. 3. As in Fig. 2: Mean and std dev of (a),(b) HOAPS-3 wind speed (m s^{-1}), (c),(d) air–sea humidity difference (g kg^{-1}), (e),(f) near-surface air humidity (g kg^{-1}), and (g),(h) SST (°C).

1170 mm yr^{-1} (Angelucci et al. 1998; Boukthir and Barnier 2000; Mariotti et al. 2002).

The precipitation estimate from HOAPS-3 is lower than observational values (310–700 mm yr^{-1}) derived mainly from coastal rain gauges and some midsea satellite retrievals (310–770 mm yr^{-1}) and is also lower than NCEP and ERA reanalysis estimates (320–500 mm yr^{-1}). The lower precipitation estimates from HOAPS-3 will be discussed further in the next section. The midrange evaporation estimates and low precipitation estimates of HOAPS-3 place the freshwater budget satellite values in the upper range of both the observational values (420–1230 mm yr^{-1}) and the reanalysis values (590–680 mm yr^{-1}).

It is noted here that the estimates of previous studies quoted above are derived based on different types of datasets that include different sampling in their calculations of the basin-mean values. While the HOAPS dataset and satellite microwave retrievals in general exclude the coastal regions, ship data tend to also be weighted more toward the open sea areas and station data of properties such as precipitation include a coastal bias. Reanalysis data equally weigh all regions but may include secondary biases depending on the spatial distribution of the assimilated data. In any case, since reanalysis data provide complete basin coverage they can be used to test how data sampling changes the basin-mean values. The NCEP reanalysis data for the period 1989–2001 give an evaporation value of 869 mm yr^{-1} for the whole Mediterranean basin whereas, when sampled over the open-water grid points included in HOAPS, they give a value of 1168 mm yr^{-1}. This implies that the overestimate of the satellite estimate compared to previous reanalysis studies is in part a sampling issue. For precipitation, the NCEP reanalysis gives a value of 412 mm yr^{-1} for the total basin and a value of 456 mm yr^{-1} for the open water grids, implying that the HOAPS underestimate does not come from sampling but from other factors—which, as mentioned before, will be examined later in the text. In the satellite–reanalysis comparisons that will be presented in the next session, the reanalysis data are sampled at the HOAPS grid points to produce corresponding basin-mean estimates.

b. Wind speed, air humidity, and SST

Inspection of the mean state and interannual variability of the wind speed and humidity fields (Figs. 3a,c) shows that evaporation (Fig. 2c) has a tighter spatial relationship with the surface humidity difference than with the wind field, since the largest evaporation occurs in the basin (Levantine Sea) with the smallest wind speeds and the largest humidity difference. In particular, the wind pattern is dominated by localized extrema as in the large values over the Gulf of Lions (8 m s^{-1}; Fig. 3a), the Cretan Passage (7.5 m s^{-1}), and the Kasos Straits (6.5–7 m s^{-1}) on account of seasonal outbreaks. The seasonality of the extrema in wind magnitude is attested by the variance field shown in Fig. 3b, where indeed most of the variability is over the western and central basins (the Balearic, Tyrrhenian, and Ionian Seas), as well as south of Crete, and not so much in the eastern Levantine Sea.

TABLE 1. HOAPS-3 evaporation annual means (mm day^{-1}) and total uncertainties within HOAPS-3 given here as percentage of the mean for each year in the satellite record.

	Mean (mm day^{-1})	Uncertainty (% of mean, mm day^{-1})
1988	2.64	29
1989	2.45	25
1990	2.65	25
1991	2.60	33
1992	2.64	32
1993	2.73	24
1994	2.92	21
1995	2.77	24
1996	2.70	25
1997	2.72	20
1998	2.96	27
1999	2.94	18
2000	3.05	28
2001	3.11	22
2002	2.88	21
2003	3.23	28
2004	2.98	28
2005	3.16	22

On the contrary, the humidity difference between the air and the sea, which is the sea surface saturation specific humidity less the near-surface specific humidity, sets the north–south and east–west gradient of evaporation and therefore the geographical structure of the freshwater budget. Largest values of humidity difference (5.5 g kg^{-1}; Fig. 3c) are found in the Levantine Sea where the air is on average drier (Fig. 3e) compared with the air masses over the central Mediterranean Sea (3.5–4.5 g kg^{-1}). The humidity difference is smallest over the western Mediterranean (2–3.5 g kg^{-1}), particularly in the Gulf of Lions where colder SSTs (Fig. 3g) and very dry air masses (Fig. 3e) lead to minima in the air–sea humidity difference.

Values of SSTs are very similar in the eastern and central basins both in magnitude and in geographical structure and are about 2°–5°C warmer than the western basin (Fig. 3g). Specifically, the surface Mediterranean waters are warmest in the Ionian (19.5°–21°C) and Levantine basins (20°–22°C) and coldest in the Balearic Sea (17°–19°C), particularly in the Gulf of Lions. SST variability (Fig. 3h) is largest in the Ionian and the

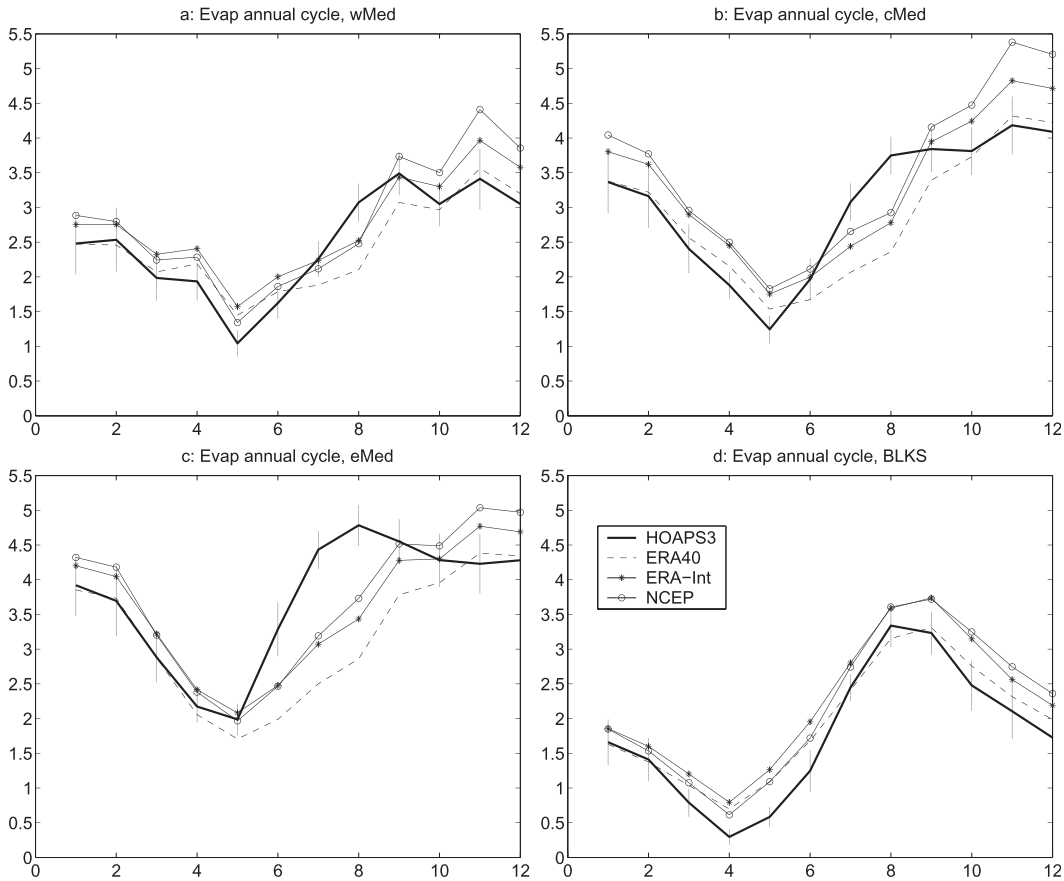

FIG. 4. Climatological mean annual cycle of evaporation (mm day^{-1}) in each basin (a) western Mediterranean (wMED), (b) central Mediterranean (cMED), (c) eastern Mediterranean (cMED), and (d) Black Sea (BLKS). Variance around the HOAPS-3 mean annual cycle is shown with vertical lines. The geographical definition of the basins is given in the beginning of section 4a.

Tyrrhenian basins and weakest in the central Levantine Sea. The easternmost part of the Mediterranean Sea also exhibits large variability.

Particularly over the Black Sea, evaporation is mainly wind driven and is largest over the western side (Fig. 2c) where the winds are stronger (Fig. 3a). The Black Sea surface climatology is influenced by the Siberian and Azores surface pressure patterns and strong, cold dry wind outbreaks occur mainly in the wintertime (Staneva and Stanev 1998). The air–sea humidity difference is small (Fig. 3c), with the surface air being usually dry (Fig. 3e) over cold waters (Fig. 3g). The large interannual changes in SST over the Black Sea will be addressed in section 4b.

In summary, the existence of the dry air over relatively very warm surface waters in the Levantine Sea results in large humidity air–sea differences and therefore large evaporation and freshwater losses from the surface ocean. In the western part of the Mediterranean, much cooler SSTs combine with moderately moist air above to reduce humidity differences between the sea surface and the surface air and therefore reduce evaporation and freshwater exchanges between the atmosphere and the sea. The central part of the basin has high sea surface temperatures underneath very moist air masses, resulting in moderately large evaporation and freshwater exchanges. The Black Sea is cold and in contact with dry air masses so that evaporation on average barely overwhelms precipitation, resulting in only slight losses of freshwater from the surface.

c. *Uncertainties within HOAPS-3*

Uncertainties in the estimates of evaporation arise from random and systematic errors in the retrievals of the variables due to sampling, instrument noise, and satellite coverage as well as in the errors introduced by calibrations and the bulk formula itself.

To examine the uncertainties associated in the HOAPS dataset, the method of Gleckler and Weare (1996) is adopted, in which it is assumed that the standard deviation of a retrieved field is entirely due to random and

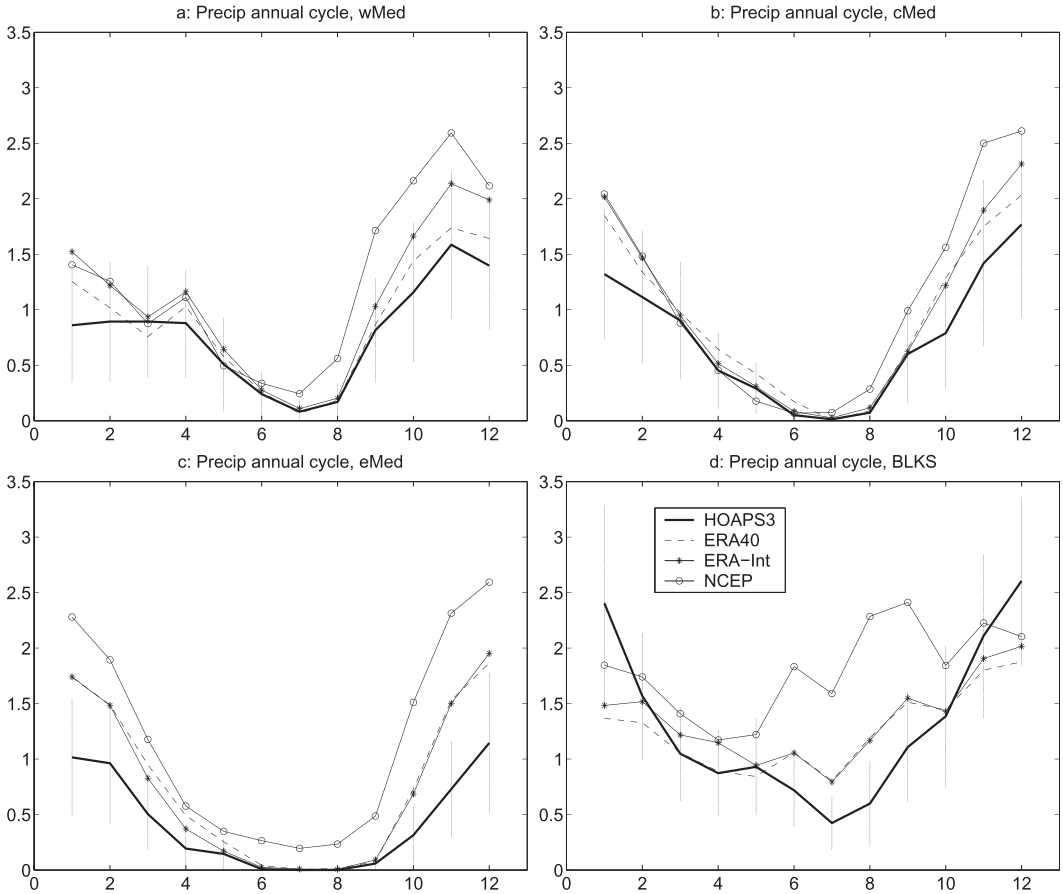

FIG. 5. As in Fig. 4, but for mean annual cycle of precipitation.

systematic errors in the retrievals–estimates. Table 1 shows the HOAPS-3 evaporation basin-mean annual uncertainties, calculated as the percent difference of each annual mean value from the 18-yr mean. It must be noted that this assumption clearly provides an upper limit of the uncertainty since part of it is the real interannual variability of the system. Keeping this in mind, the maximum uncertainty of the evaporation is 33% of the mean. The maximum uncertainty due to random errors in the constituent fields (results not shown here) is 22% of the mean for the surface wind speed, 20% for air humidity, and 18% for SST. Biases of the HOAPS-3 latent heat flux estimate from the Southampton Oceanography Center (SOC) climatology (Josey et al. 1998) over the entire Mediterranean but excluding the Black Sea are 0.63 W m^{-2}.

The analysis presented in this section introduces the satellite estimates of the Mediterranean freshwater budget climatology and quantifies the contribution of the different components and state parameters to this budget. The use of a satellite-based dataset such as HOAPS-3 is beneficial in estimating fluxes because all the fields and state parameters are measured–estimated coincidentally–colocationally and consistently used. The dataset is therefore suitable for attribution studies that reveal the physical mechanisms underlying complex processes such as the water cycle.

4. Scales of variability

In this section all datasets (HOAPS-3, ERA-40, ERA-Interim, and NCEP) are analyzed only over the regions of common coverage. This results in description of only the open-water flux variability and excludes variability in coastal and marginal seas (Adriatic and Aegean).

a. The annual cycle

The climatological mean annual cycle is examined here in the satellite and the reanalysis datasets for the period 1989–2001. The analysis is done for the four subbasins (Fig. 1): the western Mediterranean (wMED) that extends from Gibraltar to the Straits of Sicily and includes the Alboran and the Balearic Seas, the Gulf of Lions and the Tyrrhenian Sea; the central Mediterranean (cMED)

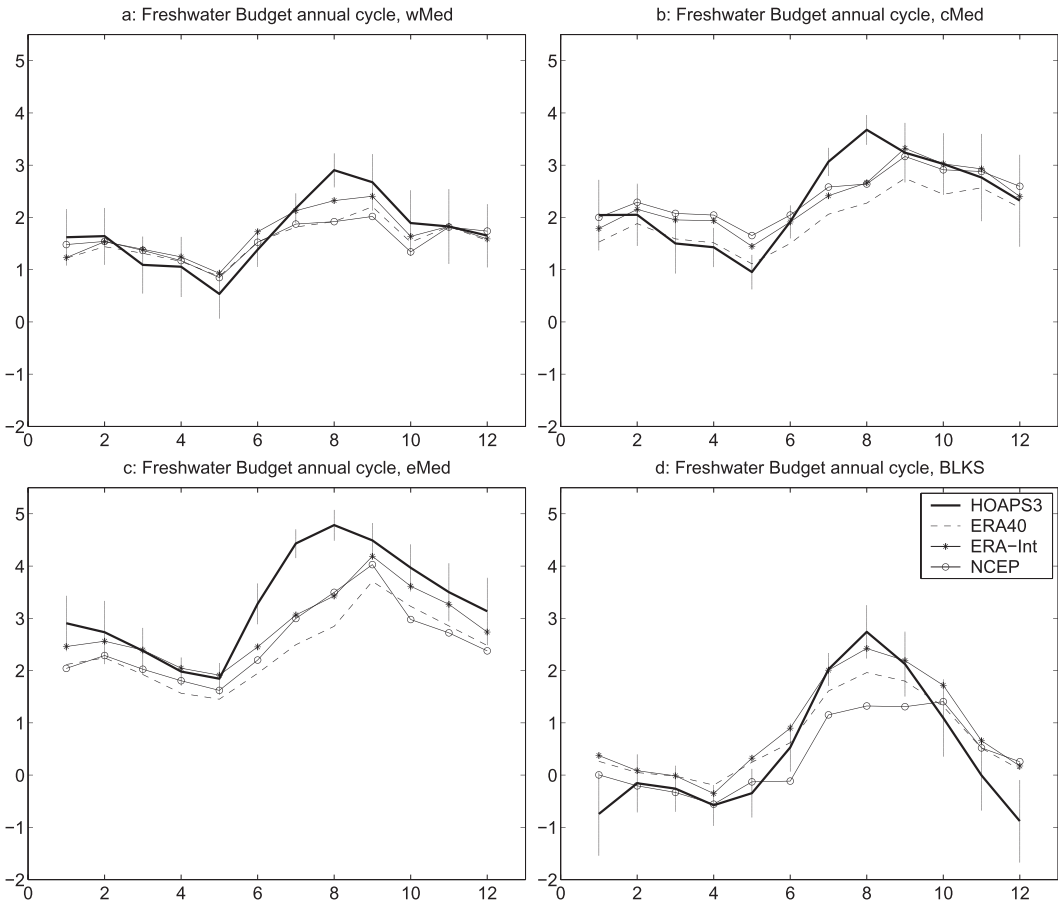

FIG. 6. As in Fig. 4, but for mean annual cycle of the freshwater budget.

that stretches below the Straits of Sicily, includes the Ionian, and ends on the western coast of Peloponnese; the eastern Mediterranean (eMED) that includes the Libyan Sea and the Levantine basin and reaches the coasts of the Middle East; and finally the Black Sea (BLKS). Also in this section, the estimates of the Mediterranean freshwater budget from the three different reanalysis datasets are presented and compared to the satellite retrievals.

All reanalysis estimates and satellite retrievals show a distinct seasonal cycle for evaporation (Fig. 4), with minimum values in the late spring and maximum values in the late fall to early winter in all four basins. Reanalyses have higher evaporation values in most basins and seasons, with the largest differences relative to HOAPS-3 occurring during the winter months (November to March) and the smallest during spring and summer. In the winter evaporation differences are 1–2 mm day^{-1} and in the spring–summer about 0–1 mm day^{-1}. This results in a stronger seasonal cycle range in the reanalysis datasets (about 4 mm day^{-1}) than in the satellite retrievals (about 3 mm day^{-1}). Only in the central and eastern Mediterranean from June–July to September are the HOAPS-3 evaporation values larger than the reanalysis values. The ERA-40 evaporation values are lower than the other two reanalysis datasets in all four basins.

Both satellite and reanalysis estimates show that rainfall attains a near-zero minimum in the summer and maxima in the winter (Fig. 5). The rainfall seasonal cycle from the reanalyses compares well with that from the satellite estimates in all basins except in the Black Sea where NCEP diverges from the other reanalyses and HOAPS-3. In the Black Sea (Fig. 5d), satellite rainfall is minimum during the summer months (June–August) while in the ERA reanalyses those minima are about 0.5 mm day^{-1} shallower; the NCEP reanalysis shows maxima in August–September.

During the winter months, the HOAPS-3 retrievals show smaller precipitation values than all the reanalysis datasets, with differences of 0.5, 1, and 1.5 mm day^{-1} in the western, central, and eastern Mediterranean, respectively. This may be due to the fact that HOAPS-3 estimates rely on SSM/I retrievals. Microwave retrievals primarily detect precipitation that falls from cold ice

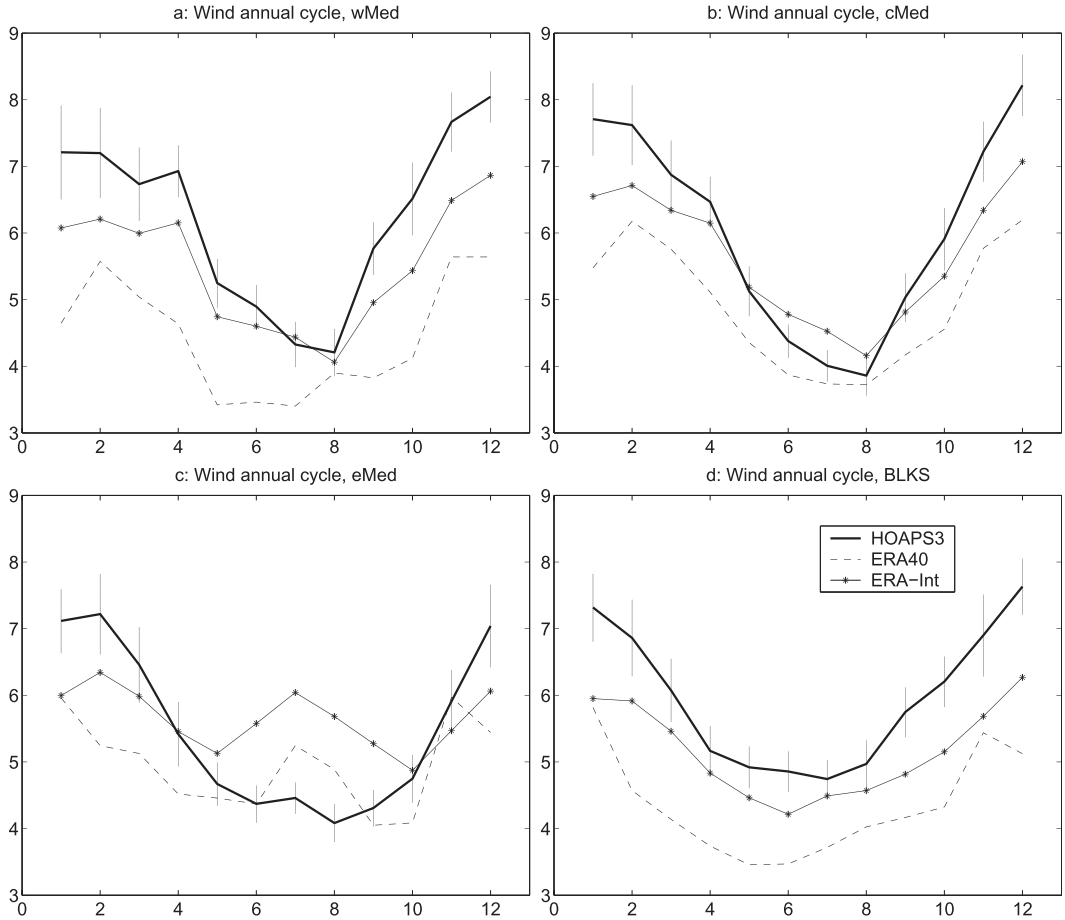

FIG. 7. As in Fig. 4, but for mean annual cycle of the near-surface wind speed (m s^{-1}).

clouds and may be missing significant amounts of precipitation falling from warm, winter stratiform clouds that often form in the vicinity of midlatitude frontal systems. Among the reanalysis datasets, values from the two ERA datasets are smaller that those from the NCEP dataset in all four basins.

Consequently, the freshwater budget exhibits a seasonal cycle with minimum values in the late spring and maximum values in the late summer in both reanalysis and satellite estimates (Fig. 6). The minimum is caused by the small evaporation values in late spring and the maximum by the small precipitation values in late summer. The differences in evaporation and precipitation seasonal cycles are largest during summer and early fall months, especially in the eastern Mediterranean (Fig. 6c) because of the evaporation differences there (Fig. 4c) and in the Black Sea because of precipitation differences (Fig. 5d).

To help explain the disagreement between the satellite and reanalysis evaporation fluxes, we examine the input variables to the bulk flux formula. From the fields that constitute evaporation, air humidity and SST show small differences between reanalysis and HOAPS-3 values (results not shown here) for all regions except the eastern Mediterranean during June to September, where satellite air humidity is on average 3 g kg^{-1} less than all reanalysis estimates. Wind magnitude differences, however, are significant (Figs. 7a–c). Wind speed is significantly lower in ERA-40 than the HOAPS-3 retrievals, whereas ERA-Interim exhibits wind speed values and seasonal variability similar to those of the satellite retrievals in all the basins except the eastern Mediterranean during summer–early fall. There, the HOAPS-3 wind field is characterized by winter maxima and summer minima whereas all reanalyses show a weak (ERA-40) or more pronounced (ERA-Interim) maximum in the summer and equivalent large values in the winter. Wind speeds over the Levantine basin (i.e., east of Crete and to the south of Turkey and Cyprus) are generally more pronounced in the reanalysis datasets than in HOAPS-3. Nevertheless, the differences in the summer winds and air humidity compensate to produce

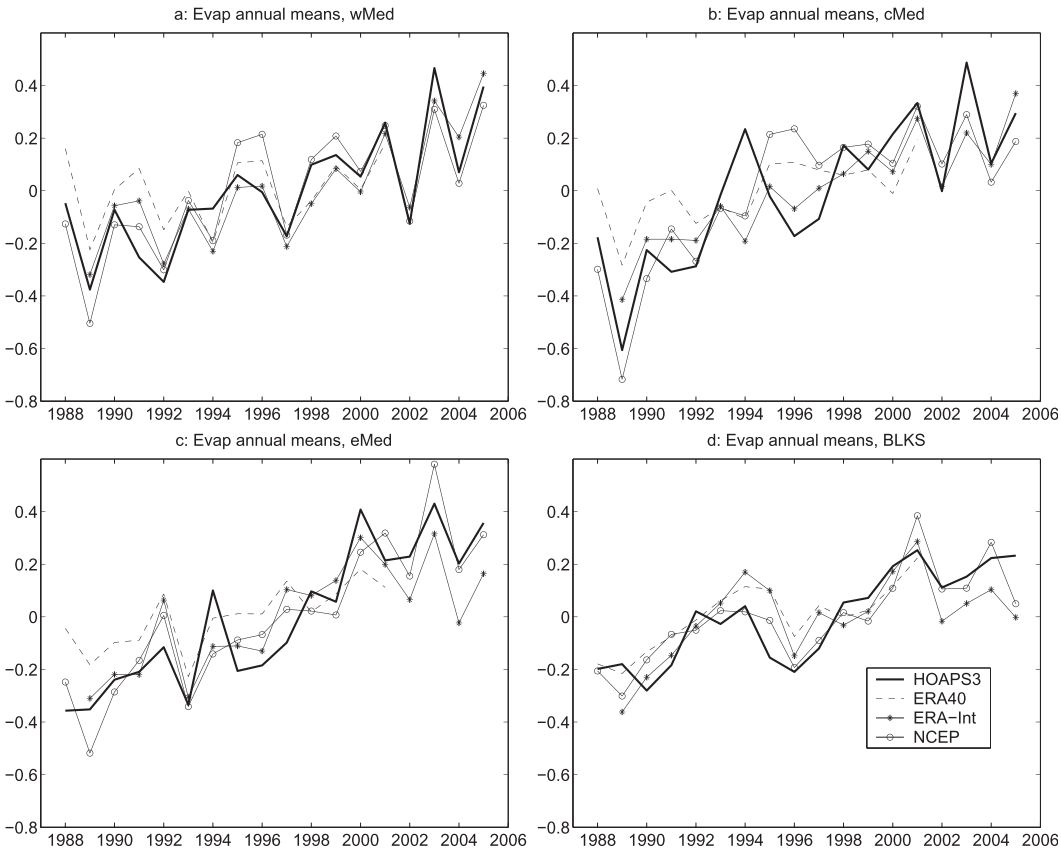

FIG. 8. Annual mean evaporation anomalies (mm day^{-1}) averaged over different regions: (a) wMed, (b) cMed, (c) eMed, and (d) BLKS. Anomalies were computed from the raw time series at each grid point after the each dataset climatological mean annual cycle was removed.

evaporation fields with greater agreement between the reanalysis and satellite estimates.

b. Interannual variability

The substantial changes in the freshwater budget in the Mediterranean region have been examined previously using reanalysis and in situ measurements (e.g., Béthoux and Gentili 1999; Boukthir and Barnier 2000; Mariotti et al. 2002). Here we derive the HOAPS-3 estimates of freshwater flux variability for the period 1988–2006 and compare them with the three reanalysis datasets. In the following, flux and other variable anomalies are computed by removing the climatological mean annual cycle from the monthly time series. Comparisons are made only over the common grid in the satellite and reanalysis data that corresponds to the HOAPS-3 grid (i.e., over open water only, excluding coastal regions and the Adriatic and Aegean Seas).

Over the period 1988–2006, evaporation (Fig. 8) has been increasing over the Mediterranean and the Black Seas with similar rates in all the basins even though the year-to-year variability may differ. The trends in the Black Sea are slightly less than those in the other basins. The statistical significance (Mann–Kendall test) for the evaporation trends is above 95% in all basins. The reanalyses agree well with the satellite data in the overall trends although the uncertainties in each year are different. The two ECMWF reanalyses agree better with the satellite data in all the basins except for the period 1994–96.

Over the same period, rainfall rates show no discernible trends except in the western Mediterranean, which experienced small increases (Fig. 9), and the Black Sea, which experienced small decreases, but these trends are not statistically significant. Generally, the reanalyses agree well with the satellite data on the overall trends, although the amplitude of the year-to-year variability is more pronounced in the reanalyses, especially in the eastern Mediterranean, and less so in the central Mediterranean and the Black Sea. The ERA-Interim reanalyses compare fairly well with the HOAPS-3 dataset whereas the NCEP reanalysis shows substantial differences.

As a result mainly of the evaporation trends, the freshwater deficit in the Mediterranean over the period of

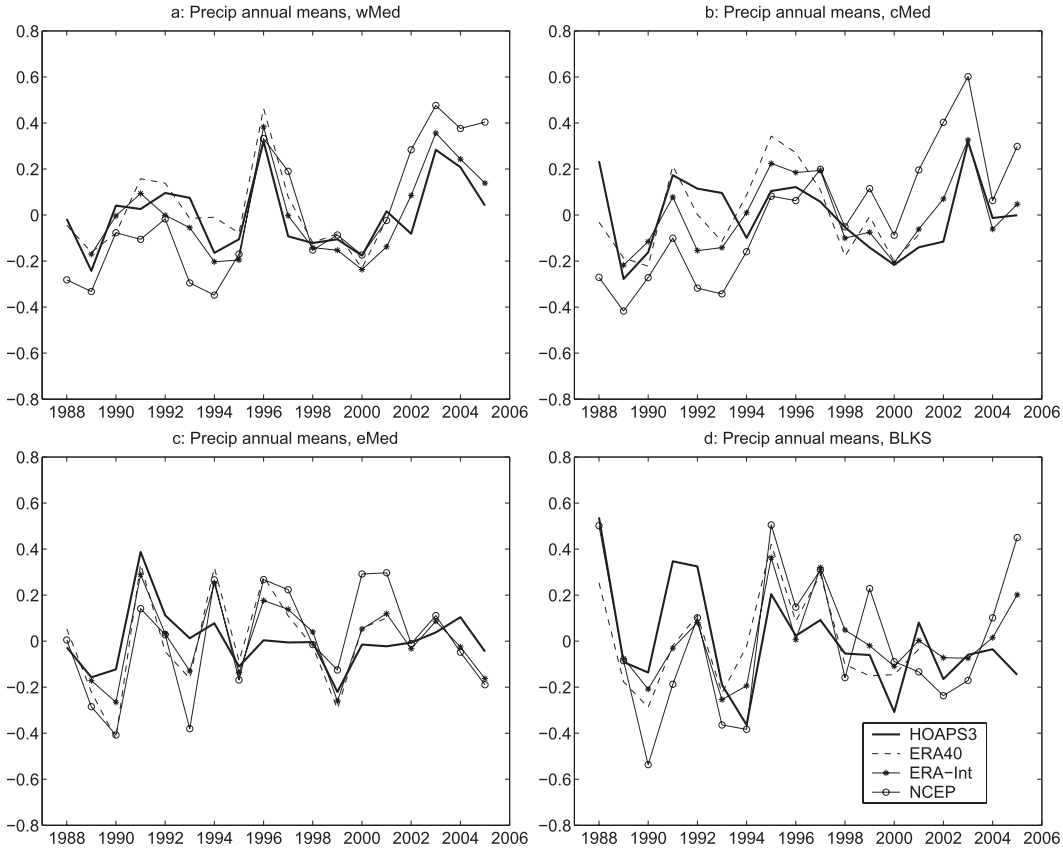

FIG. 9. As in Fig. 8, but for annual mean precipitation anomalies (mm day^{-1}).

1988–2005 has been increasing by 0.2–1.5 mm day^{-1} yr^{-1} over the entire basin, with the smallest increases occurring over the western Mediterranean basin and the largest over the eastern basin (Fig. 10) and the Black Sea. Again, the Mann–Kendall test shows that these trends are statistically significant above the 95% level. These increases are driven by the evaporation trends, which are more pronounced in the central and eastern Mediterranean and less pronounced in the western part. At the same time, rainfall has been increasing in the western Mediterranean by about 0.2–0.6 mm day^{-1} yr^{-1} (not a statistically significant trend) counteracting the increases in the evaporation whereas the role of rainfall over the most of central and eastern Mediterranean is small.

To explain the evaporation increases that drive the freshwater deficit increase in most Mediterranean basins, the trends of the state parameters that affect evaporation are examined. Figures 11–13 show the trends of wind speed, air humidity, and SST in the four basins for HOAPS-3 and the three reanalysis datasets. Wind speed shows increasing trend (Fig. 11) that is more pronounced in the western Mediterranean and less so in the other basins. The trend is present in both the HOAPS-3 and the reanalysis datasets, although in HOAPS-3 the wind speed values are very low during the earlier part of the record (1988–91). This is possibly due to low satellite coverage during those years as only one (partly defective) SSM/I (on *DMSP-F08*) was in space at that time. These trends are statistically significant above 95% only in the Black Sea, although in all other basins the statistical significance is above 90%.

Surface air humidity (Fig. 12) does not show obvious trends with the exception of the eastern Mediterranean, where it shows a slight increase that is statistically significant at the 90% but not the 95% level. SST shows strong but not statistically significant increasing trends in all the basins (Fig. 13) except in eastern Mediterranean, where the statistical significance is above 95%. Comparison of Figs. 11–13 shows that the driving mechanism for the interannual trends in the evaporation (and thus the freshwater deficit) is different for different basins. In the central and eastern basins as well as in the Black Sea, SST warming is more pronounced and drives large air–sea flux changes, while the wind speed increases play a secondary role. On the other hand, in the western

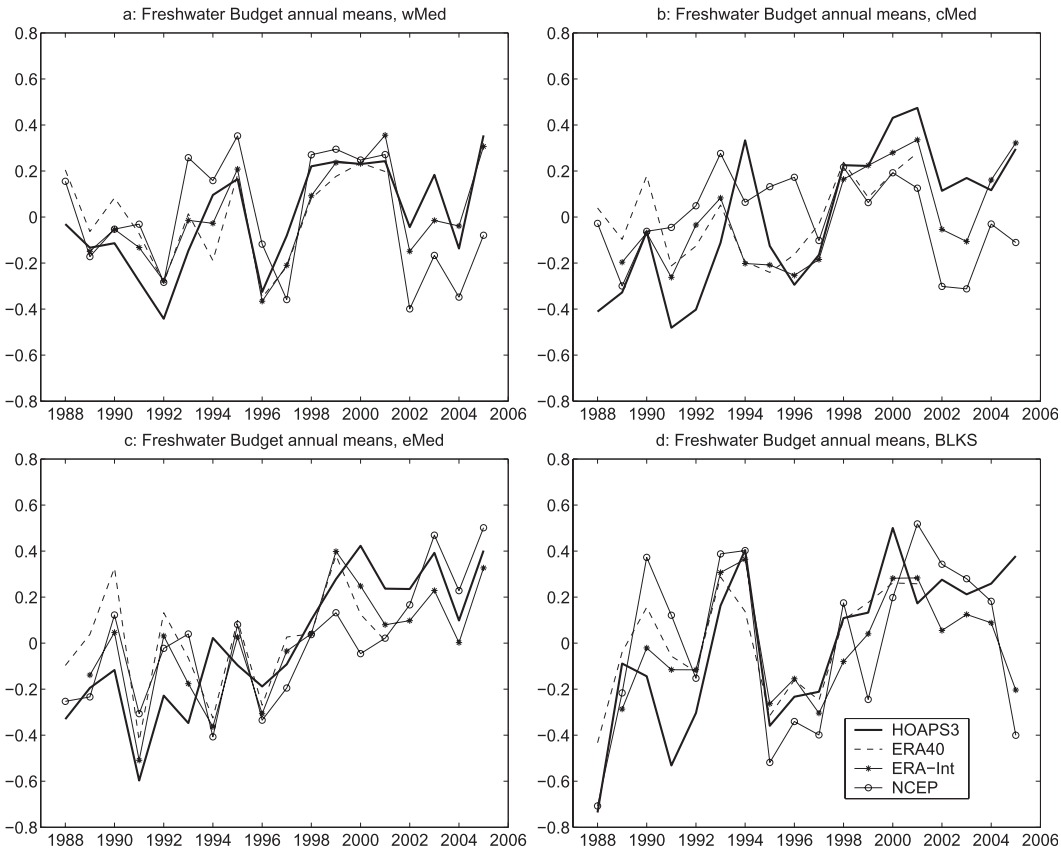

FIG. 10. As in Fig. 8, but for annual mean freshwater budget (mm day^{-1}) anomalies.

Mediterranean the driving mechanism is mostly dynamic (i.e., an increase in the wind driven heat losses at the surface, with little increase in SST).

The interannual trends discussed in this section are summarized in Table 2, along with the percentage of the coverage in the basin that these trends are above the 95% significance level. It is shown that the freshwater budget trends are due mostly to trends in the evaporation. Precipitation changes are reinforcing freshwater deficit increases in all basins except the western Mediterranean, although the precipitation trends are not statistically significant. Additionally, the trends in evaporation are mostly due to the humidity differences (which are due to SST trends) in the eastern Mediterranean and the Black Sea and to wind variability in the western Mediterranean. In the central Mediterranean, wind and SST both exhibit increasing trends.

c. *NAO and the Mediterranean freshwater flux*

The North Atlantic Oscillation (NAO) is the seesaw in atmospheric pressure between the subtropical high and the polar low (Hurrell 1995). The NAO represents the dominant mode of wintertime variability in the North Atlantic and through teleconnections in the adjacent regions. The wintertime [December–February (DJF)] NAO index over the period of interest (1988–2002) exhibited a mostly positive phase during the earlier part of the record (1988–94) and alternating positive/negative phases after 1995 (Fig. 14a). Andersson et al. (2010) found that HOAPS-3 precipitation patterns strongly relate to the state of the NAO. Here, the HOAPS-3 freshwater budget and its major components are examined with respect to their dependence on NAO-related variability.

Wintertime evaporation anomalies are found to be weakly correlated with NAO except in the western Black Sea region (Fig. 14b). On the contrary, wintertime precipitation anomalies are anticorrelated with NAO over the western Mediterranean and in the northern part of the central Mediterranean (Fig. 14c); that is, winters with positive NAO phase are drier than winters in the negative NAO phase, as was also found by Mariotti et al. (2002) and Andersson et al. (2010). As a result, the freshwater deficit ($E - P$) is positively correlated with NAO phases over the western basin (Balearic Sea) and the central basin (Ionian Sea) (Fig. 14d) mostly through

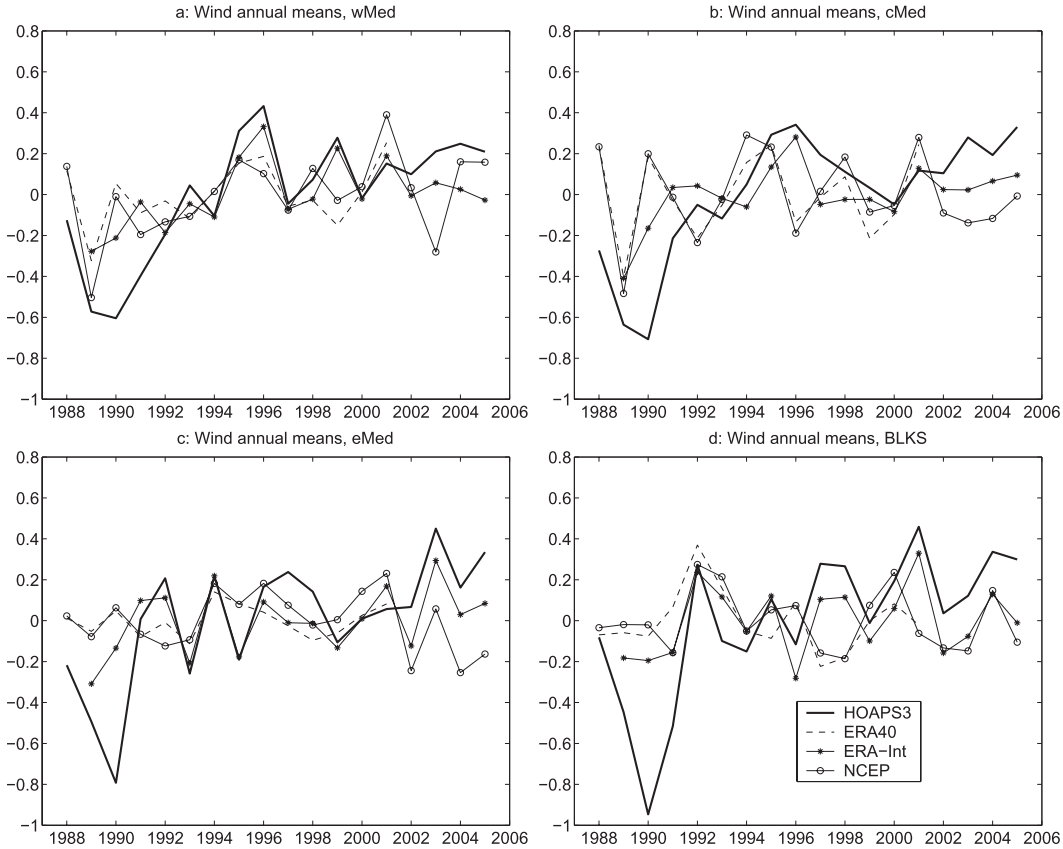

FIG. 11. As in Fig. 8, but for annual mean near-surface wind speed (m s^{-1}) anomalies.

precipitation and less so through evaporation. This result implies that during negative NAO phase winters, increased precipitation and therefore increased freshwater input into the sea surface over the western and central Mediterranean may hinder wintertime surface buoyancy losses and possibly deep–intermediate water formation. Events of reduced convection in the central Mediterranean are described in Roether et al. (1996). The eastern basin is not affected by the NAO, as implied by the low correlations in E, P, and $E - P$.

The significant anticorrelation patterns between evaporation and NAO in the Black Sea are mostly set by the wind and less so by the humidity difference (Figs. 14e,f). Northward wind pattern shifts associated with positive NAO lead to decreased evaporation in the Black Sea (Fig. 14c).

SST is more strongly anticorrelated with NAO (Fig. 14h) than the surface air humidity (Fig. 14g) throughout the Mediterranean and the Black Sea, but their combined effect produces a humidity difference field that is correlated with NAO (Fig. 14f) only over the western and central Mediterranean. Weak NAO correlations with wind and humidity difference result in evaporation essentially uncorrelated with NAO over the eastern basin.

5. Discussion

The present study demonstrates the usefulness of a state-of-the-art satellite-derived ocean surface flux product (HOAPS-3) in examining the mean properties and the variability of the ocean surface freshwater budget in the Mediterranean and Black Seas as well as in the subbasins. The study describes the differences with freshwater fluxes determined from the reanalysis datasets and indicates sources of the discrepancies relative to HOAPS-3.

The satellite-based analysis shows a freshwater deficit in the Mediterranean and Black Seas that averages 2.5 mm day^{-1} but with a significant east–west asymmetry ranging from 3.5 mm day^{-1} in the eastern part of the basin to about 1.5 mm day^{-1} in the western part. The basin mean value translates to an annual freshwater deficit about 900 mm yr^{-1}, which places the satellite estimate in the middle of the range derived by studies using in situ observations and reanalysis data: Boukthir

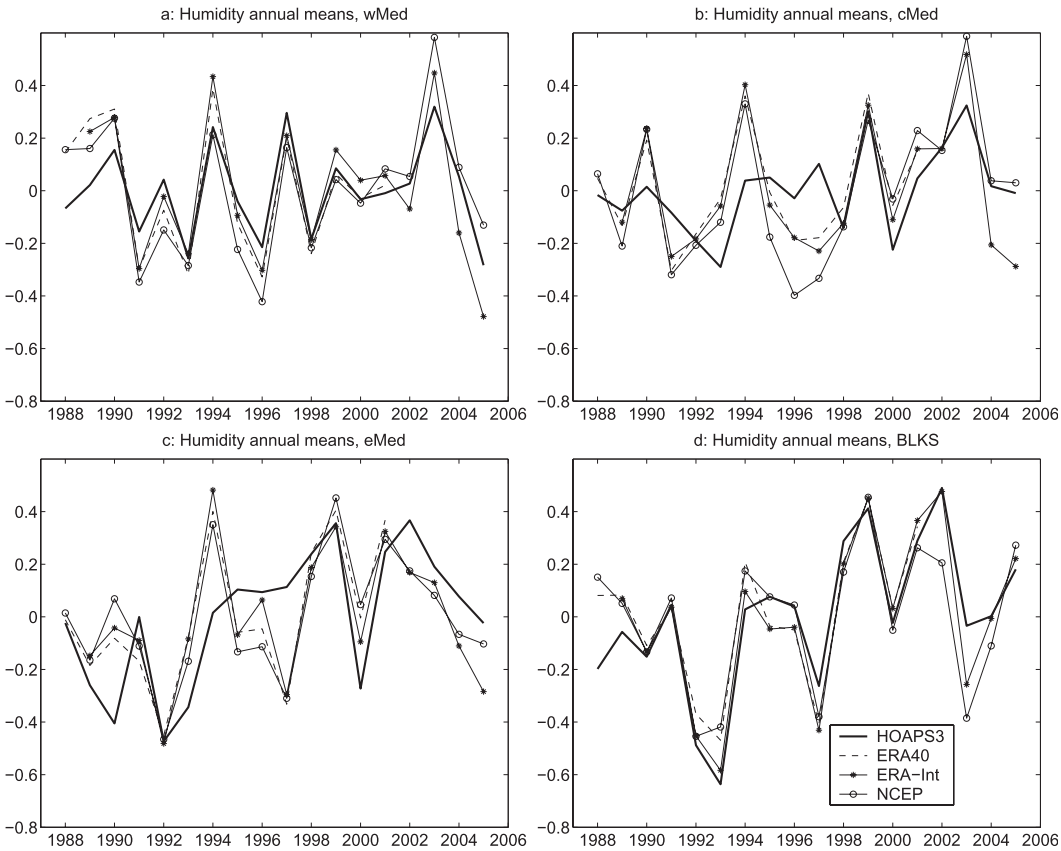

FIG. 12. As in Fig. 8, but for annual mean near-surface air humidity (g kg^{-1}) anomalies.

and Barnier (2000) reported mean values of about 650 mm yr^{-1} and Mariotti et al. (2002) values from 500 to 700 mm yr^{-1}, and Béthoux and Gentili (1999) in a review of a number of studies reported values in the range of 1050–1230 mm yr^{-1}.

Missing values in the satellite fluxes near the coasts, which are attributed to contamination of emission from land, allow only for partial coverage of the Mediterranean and the Black Seas. Budgets here are shown only for the common area coverage in the datasets used, which corresponds to open-water areas only, excluding coastal regions and marginal seas (e.g., the Adriatic and Aegean Seas).

The analysis shows that the zonal asymmetry in the water deficit is driven by evaporation differences that are determined by variability in the air–sea humidity difference in the different parts of the Mediterranean basin. The eastern Mediterranean has the largest evaporation flux thanks to a combination of high SST and low air humidity values. Freshwater deficit is smallest in the western Mediterranean and the Black Seas, where evaporation is smallest and SSTs are colder, while surface air is substantially drier over the Black Sea. Over the central and eastern Mediterranean evaporation is largest and SSTs are warmest, although the surface air is drier over the eastern basin. However, over the two basins precipitation patterns are substantially different, leading to larger freshwater loses over the eastern than over the central Mediterranean.

The trend analysis for the Mediterranean shows that the freshwater deficit increases during the period 1988–2005. The increase in freshwater deficit, which is most prominent in the eastern part of the basin, is driven by increases in evaporation that are associated in turn with increases in SST. Precipitation does not show any consistent trend during this period. Mariotti et al. (2002) found an increase in the Mediterranean water deficit in the 1948–98 period that was due to a decrease in precipitation attributed to the positive anomalies that have dominated the NAO index since the early seventies. This implies that the recent increase in the freshwater deficit has a more local thermodynamic control, whereas the increase in the earlier portion of the period was driven by large-scale dynamical processes related to the NAO.

To obtain a measure of the uncertainty in the flux estimates and the component fields, we derive the interdataset

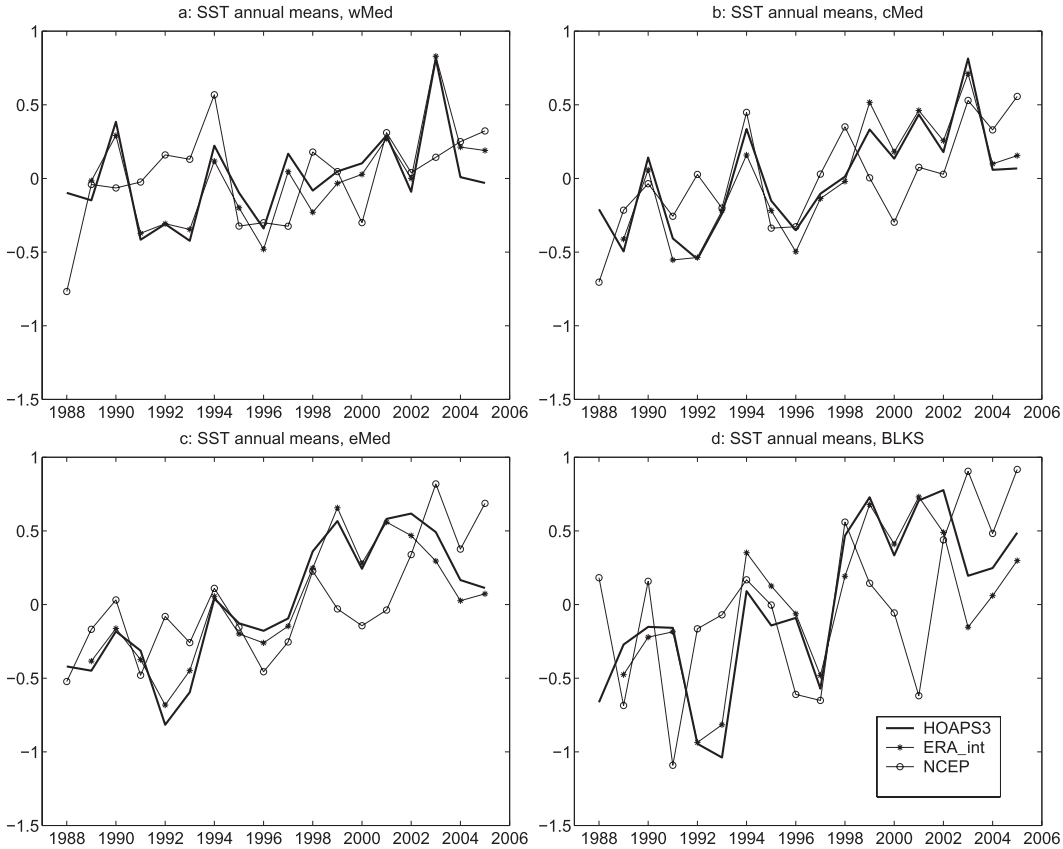

FIG. 13. As in Fig. 8, but for annual mean SST (°C) anomalies.

spread for the four datasets used in this study (HOAPS-3, ERA-40, ERA-Interim, and NCEP). The interdataset spread is computed as the standard deviation of each dataset's estimate of the seasonal (Figs. 4–7) and interannual (Figs. 8–13) variability in each region, and the results are presented in Table 3 as percent differences from the mean value. The uncertainty estimates calculated this way are lower for the interannual variability than for the annual cycle, with precipitation and surface wind speed showing the highest uncertainty values. Generally, the uncertainties are higher in the eastern basin and in the Black Sea. Freshwater budget uncertainties are lower than precipitation uncertainties, possibly due to error compensation between evaporation and precipitation in all the basins, since evaporation and precipitation contribute to the budget with opposite signs. The lower uncertainties in humidity and SST may be attributed to the fact that reanalysis and satellite data use similar datasets for these quantities. The interdataset spreads presented here point to the need for more independent data sources (in situ measurements, different satellite platforms, different bulk parameterizations) in

TABLE 2. Interannual trends based on monthly mean anomalies for each flux and variable from the HOAPS dataset. Rightmost column shows the percentage of the basin coverage (number of grid points over total number of grid points) where these trends are above the 95% significance level.

	wMED	cMED	eMED	BLKS	Area above 95% sig. level
EVAP (mm day^{-1} yr^{-1})	0.04	0.04	0.04	0.03	98.9%
PRECIP (mm day^{-1} yr^{-1})	0.01	−0.002	−0.001	−0.02	5%
BUDG (mm day^{-1} yr^{-1})	0.02	0.04	0.05	0.05	73.7%
WIND (m s^{-1} yr^{-1})	0.04	0.04	0.04	0.05	100%
AIR HUMID. (g kg^{-1} yr^{-1})	0.001	0.01	0.03	0.03	49.7%
DHUM (g kg^{-1} yr^{-1})	0.02	0.03	0.04	0.02	91.7%
SST (°C yr^{-1})	0.02	0.04	0.06	0.07	86.5%

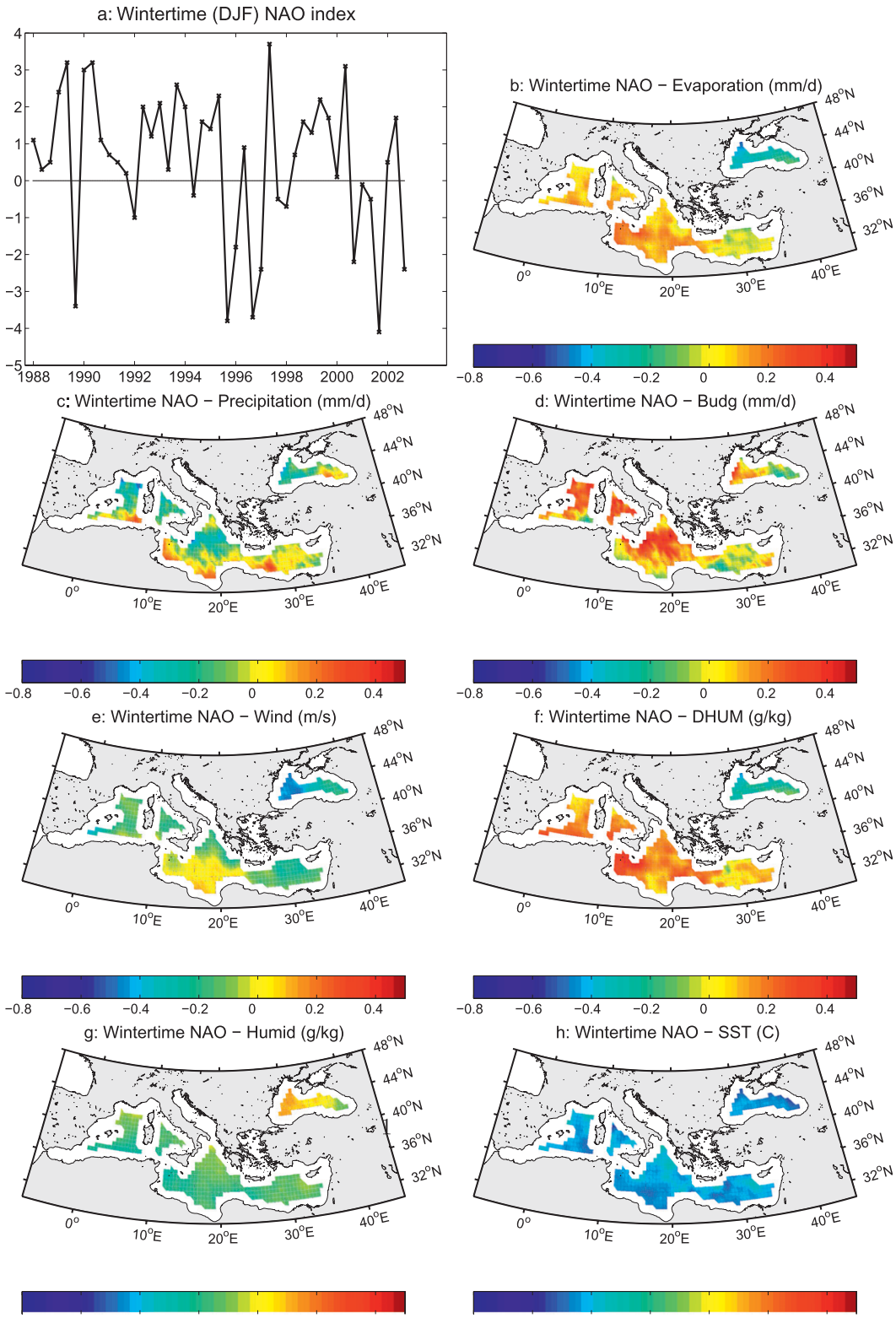

FIG. 14. Wintertime correlations between (a) NAO index and the anomalies in each HOAPS-3 field: (b) freshwater budget, (c) evaporation, (d) precipitation, (e) wind speed, (f) humidity difference, (g) surface air humidity, and (h) SST.

TABLE 3. Uncertainties (= interdataset spread = standard deviation as percentage of the mean) in the estimate of the regional fluxes from the datasets used in the present study (HOAPS-3, ERA-40, ERA-Interim, and NCEP) and for the period 1989–2001.

	Field	Entire Med.	wMED	cMED	eMED	BLKS
Seasonal	EVAP	16	17	20	25	29
	PRECIP	42	43	43	48	56
	BUDG	22	21	22	26	32
	WIND	15	22	15	16	22
	AIRHUM	9	9	9	11	11
	SST	2	3	2	2	4
Interannual	EVAP	9	11	11	9	14
	PRECIP	30	34	32	47	30
	BUDG	17	20	15	22	29
	WIND	19	27	20	17	27
	AIRHUM	4	5	3	5	9
	SST	3	5	3	3	5

order to reduce the uncertainties in our knowledge of the surface energy fluxes.

In general, the reanalysis datasets tend to have higher evaporation values in most parts of the basin, while they agree well with the satellite retrievals of the annual cycle of evaporation, precipitation, and freshwater. The ERA-Interim improves the agreement with the satellite retrievals relative to the ERA-40, in large part because of an improvement in the representation of the wind speed field. These differences in freshwater fluxes constitute an uncertainty range that must be accounted for in modeling studies of the Mediterranean region that use surface freshwater forcing to simulate oceanic preconditioning of deep and intermediate convection, water mass formation, and the Eastern Mediterranean Transient.

A more thorough way to establish uncertainty ranges in flux estimates due to different bulk formulations in satellite retrievals, reanalyses, and model output is to use simulator-type software that computes the fluxes given the same bulk formula and input variables at the same spatial and temporal intervals. This has been proposed by the SeaFlux group (Curry et al. 2004) and successfully demonstrated in cloud model evaluations [e.g., the International Satellite Cloud Climatology Project (ISCCP) simulator; Williams and Tselioudis 2007].

This study shows that with regards to the water cycle over open water, the Mediterranean Sea comprises three distinct basins with different behavior and variability: the western, central, and eastern basins. The Black Sea also displays a substantially different response in the seasonal and interannual trends. It is therefore suggested that turbulent fluxes over the Mediterranean are not treated as one average over the basin but are examined separately over each subbasin.

While satellite-derived ocean surface fluxes show substantial promise to improve understanding of the freshwater flux in the Mediterranean and Black Seas, comparison with in situ measurements is needed to improve confidence in the satellite-derived values. Also, the inability of satellites to accurately sense regions near the coast points to the need for a synthesis of satellite and reanalysis surface fluxes.

Acknowledgments. The authors wish to thank the project groups at the Hamburg Ocean Atmosphere Parameters and Fluxes from Satellite Data Center, the European Centre for Medium-Range Weather Forecasts, and the NOAA National Center for Environmental Prediction for making their datasets readily available for this study, and Prof. D. A. Metaxas for useful discussions. NAO Index data were provided by the Climate Analysis Section, NCAR, Boulder, Colorado. A significant part of the work was carried out at the Centre of Atmospheric Physics and Climatology at the Academy of Athens in Greece. Funding was partially provided by the NASA Energy and Water Cycle Study program under NASA NEWS Grant GIT G-35-C56-G1. NCEP Reanalysis–derived data were provided by the NOAA/OAR/ESRL PSD, Boulder, Colorado, from their Web site (available online at http://www.esrl.noaa.gov/psd/).

REFERENCES

Andersson, A., 2009: The HOAPS climatology—Evaluation and applications. Ph.D. thesis, Universtät Hamburg, 192 pp.

——, S. Bakan, and H. Grassl, 2010: Satellite derived precipitation and freshwater flux variability and its dependence on the North Atlantic oscillation. *Tellus,* **62A,** 453–468.

Angelucci, M. G., N. Pinardi, and S. Castellari, 1998: Air–sea fluxes from operational analyses fields: Intercomparison between ECMWF and NCEP analyses over the Mediterranean area. *Phys. Chem. Earth,* **23,** 569–574.

Bengtsson, L., K. Hodges, and E. Roeckner, 2006: Storm tracks and climate change. *J. Climate,* **19,** 3518–3543.

Berrisford, P., D. Dee, K. Fielding, M. Fuentes, P. Kallberg, S. Kobayashi, and S. Uppala, 2009: The Era-Interim archive. ECMWF Tech. Rep. 1, 20 pp.

Béthoux, J. P., and B. Gentili, 1999: Functioning of the Mediterranean Sea: Past and present changes related to freshwater input and climatic changes. *J. Mar. Syst.,* **20,** 33–47.

Boukthir, M., and B. Barnier, 2000: Seasonal and inter-annual variations in the surface freshwater flux in the Mediterranean Sea from the ECMWF re-analysis project. *J. Mar. Syst.,* **24,** 343–354.

Bourras, D., 2006: Comparison of five satellite-derived latent heat flux products to moored buoy data. *J. Climate,* **19,** 6291–6313.

Castellari, S., N. Pinardi, and K. Leaman, 1998: A model study of air–sea interactions in the Mediterranean Sea. *J. Mar. Syst.,* **18,** 89–114.

Chou, S.-H., E. Nelkin, J. Ardizzone, and R. M. Atlas, 2004: A comparison of latent heat fluxes over global oceans for four flux products. *J. Climate,* **17,** 3973–3989.

Curry, J. A., and Coauthors, 2004: Seaflux. *Bull. Amer. Meteor. Soc.,* **85,** 409–424.

Fairall, C., E. F. Bradley, D. P. Rogers, J. B. Edson, and G. S. Young, 1996: Bulk parameterization of air–sea fluxes for the Tropical Ocean–Global Atmosphere Coupled Ocean–Atmosphere Response Experiment. *J. Geophys. Res.,* **101,** 3747–3764.

Gilman, C., and C. Garrett, 1994: Heat flux parameterizations for the Mediterranean Sea: The role of atmospheric aerosols and constraints from the water budget. *J. Geophys. Res.,* **99,** 5119–5134.

Giorgi, F., 2002: Variability and trends of sub-continental scale surface climate in the twentieth century. Part I: Observations. *Climate Dyn.,* **18,** 675–691.

Gleckler, P. J., and B. C. Weare, 1996: Uncertainties in the global ocean surface heat flux climatologies derived from ship observations. *J. Climate,* **10,** 2764–2781.

Grassl, H., V. Jost, R. Kumar, J. Schulz, P. Bauer, and P. Schluessel, 2000: The Hamburg ocean–atmosphere parameters and fluxes from satellite data (HOAPS): A climatological atlas of satellite-derived air–sea interaction parameters over the oceans. MPI Tech. Rep. 312, 95 pp.

Hurrell, J., 1995: Decadal trends in the North Atlantic Oscillation: Regional temperatures and precipitation. *Science,* **269,** 676–679.

Josey, S. A., 2003: Changes in the heat and freshwater forcing of the eastern Mediterranean and their influence on deep water formation. *J. Geophys. Res.,* **108,** 3237, doi:10.1029/2003JC001778.

——, E. C. Kent, and P. K. Taylor, 1998: The Southampton Oceanography Centre (SOC) ocean–atmosphere heat, momentum and freshwater flux atlas. SOC Tech. Rep. 6, 30 pp.

Kalnay, E., and Coauthors, 1996: The NCEP/NCAR 40-Year Reanalysis Project. *Bull. Amer. Meteor. Soc.,* **77,** 437–470.

Luterbacher, J., and Coauthors, 2006: Mediterranean climate variability over the last centuries: A review. *Mediterranean Climate Variability,* P. Lionello, P. Malanotte-Rizzoli, and R. Boscolo, Eds., Elsevier, 27–148.

Mariotti, A., M. Struglia, N. Zeng, and K.-M. Lau, 2002: The hydrological cycle in the Mediterranean region and implications for the water budget of the Mediterranean Sea. *J. Climate,* **15,** 1674–1690.

Peixoto, J. P., M. D. Almeida, R. D. Rosen, and D. A. Salstein, 1982: Atmospheric moisture transport and the water balance of the Mediterranean Sea. *Water Resour. Res.,* **18,** 83–90.

Raisanen, J., 2002: CO_2-induced changes in interannual temperature and precipitation variability in 19 CMIP2 experiments. *J. Climate,* **15,** 2395–2411.

Roether, W., B. Manca, B. Klein, D. Bregant, D. Georgopoulos, V. Beitzel, V. Kovacevic, and A. Luchetta, 1996: Recent changes in eastern Mediterranean deep waters. *Science,* **271,** 333–335.

Rubino, A., and D. Hainbucher, 2007: A large abrupt change in the abyssal water masses of the eastern Mediterranean. *Geophys. Res. Lett.,* **34,** L23607, doi:10.1029/2007GL031737.

Staneva, J., and E. Stanev, 1998: Oceanic response to atmospheric forcing derived from different climatic data sets: Intercomparison study for the Black Sea. *Oceanol. Acta,* **21,** 393–417.

Uppala, S., and Coauthors, 2005: The ERA-40 re-analysis. *Quart. J. Roy. Meteor. Soc.,* **131,** 2961–3012.

Williams, K., and G. Tselioudis, 2007: GCM intercomparison of global cloud regimes: Present-day evaluation and climate change response. *Climate Dyn.,* **29,** 231–250.